Paper submitted to the Journal of Geotechnical and Geoenvironmental Engineering

Three-dimensional effects observed in an internally braced excavation in soft clay

J. Tanner Blackburn[1], M. ASCE, and Richard J. Finno[2], M. ASCE

ABSTRACT

Several three-dimensional effects were observed in the performance monitoring data collected during excavation for the Ford Engineering Design Center (FEDC) in Evanston, Illinois. These responses are related to lateral deformations of the soil around the excavation walls, forces in the cross-lot and diagonal bracing that supported the temporary wall and effects on an adjacent building. These responses are presented and compared with results from current design method predictions. The excavator removed the soil in a non-uniform excavation process which impacted the forces in the internal braces. Results of three-dimensional finite element simulations of the excavation process are presented to evaluate the effects of properly modeling adjacent structures and soil elevations and accurately modeling the excavation sequence. Comparisons between calculated and observed soil deformation profiles and earth strut loading illustrate the influence of these factors on the observations.

[1] Ass't. Prof.,Zachry Department of Civil Engineering, Texas A&M University, College Station, TX 77843, jblackburn@civil.tamu.edu
[2] Prof. Department of Civil and Environmental Engineering, Northwestern University, Evanston, IL 60208, r-finno@northwesetern.edu

INTRODUCTION

A braced excavation develops well-known three-dimensional effects that cause the induced ground deformations to be smaller near the corner of an excavation wall than near its center (e.g., Bono et al. 1992; Wong and Patron 1993; Ou et al. 1993,1996, 2000; Chew et al. 1997; Lee et al. 1998; Finno and Bryson 2002; and Finno and Roboski 2005). Roboski and Finno (2005) proposed an empirical relation for the distribution of ground movements parallel to an excavation wall wherein the geometry of an excavation is related to the distribution of δ_x/δ_{Center} - where δ_x is the lateral movement at any distance *x* along a wall and δ_{Center} is the movement at the center of a wall. Perhaps somewhat less recognized is the fact that the ground deformations that occur near the center of a wall can be smaller than those associated with plane strain conditions, even when the movements develop perpendicular to the wall (Ou et al. 1993, 1996; Chew et al. 1997; Lee et al. 1998; and Lin et al. 2003). Parametric studies by Finno et al. (2006) have shown that the plane strain ratio, *PSR*, defined as the maximum lateral movement behind a wall found from the results of a 3D simulation normalized by that from a plane strain simulation depends on geometry expressed as length of wall whereat the movement is reported divided by the excavated depth, L/H_e, and length to width ratio, L/B, wall system stiffness and factor of safety against basal heave.

These case studies, parametric studies and empirical relations are valid for cases wherein the ground surface elevation is uniform around all four walls. However, three-dimensional effects for internally braced cuts can arise from different levels of ground surface retained around the excavation, the presence of adjacent basements and from non-uniform excavation procedures wherein the soil is not sequentially removed in a uniform manner. This paper presents the observed performance of the excavation for the Ford Engineering Design Center (FEDC) that illustrates these effects. The project is located on the Northwestern University campus in Evanston, Illinois and consisted of a 44 m x 37 m, internally-braced excavation with uneven initial elevations on adjacent sides. A basement of a nearby adjacent building supported on spread and strip footings impacted the stress conditions along that side of the excavation. The average depth of excavation was 8.8 m. Furthermore, space, equipment, and contractual limitations required a complex excavation sequence at the FEDC site. Corners were often excavated prior to upper support installation and access ramps were frequently placed on installed internal bracing. The unbalanced ground levels both inside and outside the excavation resulted in different patterns of lateral ground movements and unexpected distribution of forces in internal braces.

A three-dimensional finite element simulation was performed, and summarized herein, to evaluate the effects of properly modeling adjacent structures and soil elevations and accurately modeling the excavation sequence. Comparisons between calculated and observed soil deformation profiles and earth strut loading illustrate the influence of these factors on the observations.

SITE DESCRIPTION

Excavation Geometry, Stratigraphy and Support System

The FEDC excavation consisted of an approximately 8.8m deep excavation, reaching a final elevation (Evanston City Datum, ECD) of -3.8 m, supported by sheet-pile walls (XZ85) and two levels of internal bracing. Figure 1 shows a plan view and dimensions of the excavation geometry and support system. Each level of internal bracing consisted of a pair of cross-lot pipe struts, supported vertically and horizontally by a steel frame at their midpoints, and twelve diagonal braces. The loads from the retained soil were transferred to the struts via wide-flange beam walers (36Wx230 and 24Wx141). Vertical plates were welded to the sheeting and the walers so that the sheeting was in contact with the walers before the struts were installed. The struts were set in place, subjected to an axial load, and welded to the walers.

A four-story concrete and masonry building founded on shallow footings was located within 5 meters of the north wall of the excavation. The adjacent soil elevation was lower on the north side (+3.7 m, ECD), due to the building footings and an alley between the Tech Building and the excavation; the soil elevation on the east, west, and south sides of the site was approximately +5.5 m, +5.5 m, and +5.0 m ECD, respectively. The difference in elevation between two adjacent sides of the excavation influences the reaction of internal bracing support systems, as discussed later. Prior to excavation, belled caissons were installed as a deep foundation for the five-story FEDC building. The caissons were drilled from the existing grade and backfilled prior to excavation. No ground movements were recorded in the inclinometers outside the retention system as a result of the caisson installation.

Figure 2 shows the excavation support system geometry and site stratigraphy. The site stratigraphy consists of 3 to 5 meters of lake deposited sand and fill, overlying a 1 meter desiccated clay crust. Three glacially deposited clay strata, Blodgett, Deerfield, and Park Ridge, which increase in strength and stiffness with depth, exist below the clay crust and overlay a hard, gravelly clay strata, referred to as “hard pan”, at approx. elev. -16.8 m, ECD (Peck and Reed, 1954). Soil strength and stiffness properties for the Blodgett, Deerfield and Park Ridge strata were determined from a combination of standard penetration tests, cone penetration tests, vane shear testing and standard soil borings. The water table for the FEDC site consisted of water perched on the clay crust at an approximate elevation of 0 m, ECD. The bottom of the floor slab in the adjacent building was at elev. 1.5 m ECD, further adding to the lower in situ ground stresses next to the north wall.

Instrumentation

The instrumentation locations at the FEDC site are shown in Figure 1. Four slope inclinometers were installed prior to sheet-pile wall installation; two inclinometers (I-1 and I-2) are located in the alley between the excavation and the Tech Building and the remaining inclinometers were installed on the east and west sides of the site, labeled I-3 and I-5, respectively. Six permanent surveying prisms were installed on the east side of the site: 3 embedded in the surface soil (P-6,7,8), 2 placed on the sheeting (P-3,4) and one anchored to the adjacent concrete steam vault (P-5). Displacements of these points were monitored remotely on a continuous basis with an automated, radio-linked total survey station mounted on the roof of the adjacent Tech Building. Two automated, remote access tiltmeter pairs were installed on structural components of the existing Tech Building to continuously monitor building response during the excavation. Lastly, 34 vibrating wire strain gages were installed on the cross-lot and northwest diagonal bracing members, with 29 surviving the entire excavation process.

Construction Sequence

A complex excavation procedure was required due to space, equipment and contractual limitations. Soil was removed by employing a combination of large and small back-hoes and a small front loader (which could pass beneath the support struts). The use of back-hoes, rather than an exterior crane, required an access ramp for the majority of the excavation duration. To facilitate relatively efficient removal of soil under these conditions, corners were often excavated prior to upper support installation. Figure 3 presents photographs that illustrate the complex excavation sequence and placement of access ramps on top of installed support members.

The actual excavation sequence consisted of the excavation of the corners and the placement of the soil in the center of the site, prior to removal. This excavation sequence differed from the 'as-designed' excavation sequence of uniformly excavating the site to an elevation just below each layer of supports, followed by the installation of all supports at that elevation, followed by uniformly excavating the site again. The irregular excavation sequence and placement of access ramps caused loading on the support system members that was unexpected during design. Three-dimensional simulations of the excavation sequence were conducted to evaluate these effects on the soil and support system responses.

Although the excavation of the FEDC site required a complex and non-uniform excavation sequence, the excavation procedure is divided into approximate stages, listed in Table 1, for this analysis. The boundaries for these stages span several weeks of construction to illustrate the fact that the site was excavated in several corners prior to installing previous support members.

SOIL RESPONSE TO EXCAVATION

Soil deformation response during construction was monitored with four slope inclinometers and an automated total survey system. Both cantilever and deep-seated soil deformation are evident in the lateral soil profiles. Settlement and lateral movement data are obtained from the survey instrumentation.

Lateral Soil Deformation

Lateral soil displacements were monitored by weekly readings of four slope inclinometers, the locations of which are shown in Figure 1. Soil displacement perpendicular to the retaining wall can be separated into two major causes: 1) sheet-pile wall installation, causing movement away from the excavation and 2) site excavation, causing soil movement toward the excavation. Because the inclinometers were installed prior to sheeting installation, both types of soil deformation were observed.

Figure 4 shows the lateral soil movements caused by installing the sheet-pile walls. In the Blodgett and Deerfield clay strata, these movements varied from 6 to 10 mm away from the wall after installation. The equivalent thickness of the ZX85 sheeting is approximately 14 mm (defined as cross-sectional area per unit length). When installing sheeting through a saturated clay, one can expect that about half of this area will be displaced away from the wall (Finno et al. 1988). The observed wall deformation of 6 to 10 mm reflects this expected deformation (7mm).

As the FEDC excavation progressed, adjacent soil incrementally moved toward the excavation. Figure 5 shows a vector representation of incremental soil displacements in the soft clays during construction. After an initial displacement away from the walls during sheet-pile installation, the soil moved toward the excavation after wall installation; the increments correspond to the approximate stages defined in the Excavation Sequence section. The net movement into the excavation was reduced by the amount of lateral movement away from the excavation as a result of installing the sheet-pile wall.

Figures 6 and 7 show the inclinometer soil deformation profiles for inclinometer pairs 1 and 5 in the northwest corner of the excavation and pairs 2 and 3 in the northeast corner, respectively (Figure 1). These displacements were reset to zero after the wall was installed to illustrate soil deformations due to excavation. Both figures show the same pattern of movements. Lateral movements extend below the bottom of the excavation and terminate in either the stiff Park Ridge or Hardpan strata. The maximum movements occur below the bottom of the final excavated grade, and are equal to about 14 mm at inclinometers 1, 2 and 5 and 24 mm at inclinometer 3. These lateral movements correspond to normalized (by the excavated depth, H) lateral movements of 0.19% for the north, 0.14% for the west and 0.26% for the east sides of the excavation adjacent to the inclinometers.

These normalized values can be compared to those computed by empirical methods developed by Clough, et al. (1989) and Finno and Roboski (2005). The system stiffness parameter defined by Clough et al. (1989) is $(EI)/(\gamma_{water} h_{ave}^{4})$, where EI corresponds to the elastic modulus and bending moment of the wall, h_{ave} is the average spacing between support members, and γ_{water} is the unit weight of water. The system stiffness for the FEDC excavation was approximately 100. The factor of safety against basal heave, defined by Terzaghi (1967), ranged from 2.1 to 2.4 for the various depths of excavation, therefore an average value of 2.25 was employed for this comparison. MAKE CALCULATIONS FOR EACH WALL AND DEPTH – BE CONSISTENT The design chart presented by Finno and Roboski (2005) was created for flexible support systems, like that at the FEDC. The normalized lateral deformations predicted by the Clough et al. method and the Finno and Roboski methods were 0.33% and 0.16%, respectively. The value computed using Finno and Roboski's method agree well with the FEDC observed lateral deflections, especially along the north and west walls. The Clough et al. method yielded somewhat larger, although reasonable, values. The former approach could be expected to yield better results because it was based on observed performance of a flexible wall system in Chicago (Finno and Roboski 2005). ALSO, SPECULATE AS TO WHY MORE MOVEMENT ON

EAST SIDE – difference in vane shear data? Softer? i.e,. natural variations…..? In any case, the performance in terms of deep-seated movements was generally as expected for the conditions encountered at the site.

However, the movements in the upper 5 m or so were somewhat atypical, particularly when one looks at inclinometer pairs 1-5 and 2-4. The north wall inclinometers (1 and 2) experienced small cantilever movements – approximately 5 mm when the excavation reached final grade in stage 4. These small movements are representative of response of a well-constructed support system. However large cantilever movements of 35 and 28 mm were observed in the east (I-3) and west inclinometers (I-5), respectively. Furthermore, the deflected shapes of these two inclinometers indicated that the wall rotated about the second support level, rather than the first level, as is typically observed. A likely cause of these cantilever displacements is the 1.8 m higher elevation of the ground surface on the east and west sides of the excavation, as compared to the north side (see Figure 1) and the basement excavation for the building adjacent to the north side of the excavation. The cantilever movement exhibited in Inclinometer 3 and 5 implies that the diagonal bracing transfers the loads from the higher east and west sides to the lower north side and thus minimizing cantilever displacements along the north side, as indicated in data from inclinometers 1 and 2. These elevation and stress differences contributed to the smaller ground deformations in the upper 5 m of soil on the side of the excavation where excessive ground movements could have damaged the adjacent building.

Effects of movements along north wall

During the FEDC excavation, the external and internal masonry walls of the Tech Building were visually inspected for evidence of cracking. The only cracking that was observed during construction was cosmetic in the external stone and mortar façade in smaller sections of the external bearing wall, parallel to the north excavation wall. The cracks were diagonal shear and vertical tensile cracks that would correspond to “very slight” damage, according to Burland and Wroth (1978). No cracking was observed on the interior of the Tech Building.

Finno and Roboski (2005) proposed an empirically-based method for determining the settlement distribution along an excavation when given the maximum lateral or horizontal soil deformation. As shown in Figure 8, the cracking occurred at locations along the excavation where relatively large distortions are predicted. The diagonal shear cracking occurred at the inflection point of the computed settlement distribution, which is where shear strains would be expected. If it is assumed that the Tech Building did not undergo any rigid rotation, the angular distortion (differential settlement per unit length) of the section that exhibited cracking would be approximately 0.09%. This is slightly less than the critical shear strain (γ_{crit}) for masonry structures (0.11%), given by Burland and Wroth (1978); however, the critical shear strain for the external wall of the Tech Building was possible decreased due to age and weathering (Blackburn, 2005). The vertical crack in the external wall occurred at the transition point between the flat and sloped settlement distribution, which also coincided with a change in footing type (from strip to square) and footing elevation. The foundation discontinuity and transition in settlement distribution could indicate that rotation between the two segments of the Tech Building caused the vertical crack in this location (Blackburn,2005).

INTERNAL BRACING RESPONSE

Vibrating wire strain gage pairs were mounted at the quarter points of pipe supports and at the neutral axis of wide flange supports to separate bending and axial stresses. Figure 1 shows the labels and locations of the strain gage. The axial strut load, at the neutral axis, was calculated from the average of the four strain gauge readings, when all four gauges were operational. The strain gauge pairs also provided an opportunity to observe bending stress development during construction, including contributions from earth pressure, axial thermal loading, thermal bending, and construction-induced bending. The data do not include bending stresses that arise for the self-weight of the member. The strain gage sensors contained thermal sensor components, which provided strut temperature data for each data point. Support member temperature data were employed to separate the thermal and earth components of the support system response. The thermal correction procedure is modified from that proposed by Boone and Crawford (2000) and is more thoroughly described by Blackburn et al. (2005).

A summary of the maximum extreme fiber stresses in each strut is given in Figure 8. The data show that the most severe loading condition arose from the unanticipated (in design) ramp construction. Without that loading, fairly consistent trends were observed. The stresses caused by axial loads were about equal to those caused by bending. Temperature induced axial loads and bending stresses were significant and were responsible for about one-half of each component. With the exception of the ramp loading, all other causes resulted in stress levels of about 80 MPa, well below the yield stress of 250 MPa. The contractor used in-stock structural elements as the bracing, and did not attempt to optimize their size. This was fortunate given the unanticipated loading on several of the cross-lot braces by the excavator's temporary ramp.

Figure 10 presents both the total observed and calculated earth component of the axial loading of the support members during the excavation, originally presented by Blackburn, et al. (2005). The top and bottom level supports are annotated with a 'T' or 'B', respectively; and the location of each member is shown in Figure 1. Figure 10 shows that the thermal loading component of the strut force was as much as 40% of the total observed load. The earth loading of the upper level supports increased during initial excavation to -0.9 m, ECD, and stabilized after the lower level supports are installed. Loading of the lower supports continued to increase after the excavation reached final grade, eventually stabilizing 10-20 days after the final grade is reached. The axial load increase in the upper levels (T-gages) after the lower level supports (B-gages) are removed illustrates that the backfill cannot be assumed to absorb all soil loads during bracing removal. In fact, the maximum strut load was observed during this stage of the excavation, in support T-3. The maximum measured axial loads in the upper and lower support levels were consistent with axial loads predicted by employing Terzaghi and Peck's apparent pressure method (Terzaghi and Peck, 1967; Blackburn et al., 2005).

THREE-DIMENSIONAL FINITE ELEMENT ANALYSIS OF SOIL AND SUPPORT SYSTEM RESPONSE

Three-dimensional finite element simulations of the FEDC excavation were made to help explain the different deformation profiles and to evaluate the causes of the somewhat unexpected bracing responses. Given the different ground surface elevations around the walls and the presence of diagonal bracing, plane strain simulations would not adequately represent the conditions.

Model Geometry and Parameters

Plaxis 3D Foundation (Plaxis, 2004), a commercially-available geotechnical finite element software package, was employed to analyze the soil and support system response to the

FEDC site excavation. The 350m by 350m by 24.5m three-dimensional finite element mesh, used to model the entire FEDC excavation, was created by projecting a two dimensional, 350m by 350m, mesh geometry in the vertical direction. Figure 10 shows an inset of the excavation area and a cross-section of the soil stratigraphy mesh. Soil and structural elements were added and subtracted during individual calculation stages to simulate the installation of the support system and excavation process.

The six soil layers are labeled as: 1) Sand/Fill, 2)Clay crust 3) Blodgett stratum (soft clay), 4) Deerfield stratum (medium clay), 5)Park Ridge stratum (stiff, silty clay) and 6) Hardpan (hard clay, sand, gravel). All soil layers were modeled using the hardening soil model implemented in PLAXIS (Schanz, 1999). The hardening soil model is an elasto-plastic model with separate shear and volumetric yield surfaces and a Mohr-Coulomb failure criterion. Stiffness parameters are stress-level dependent. Table 2 contains the hardening soil model parameters obtained by employing inverse optimization of the FEDC excavation data (Rechea, 2006). An inverse analysis algorithm was developed by Finno and Calvello (2005) which compares the computed lateral soil deformations to observed slope inclinometer data. The automated process executes a series of several two-dimensional finite element modeling calculations, minimizing the difference between the computed and observed values so that selected parameters, in this case the secant stiffness parameter (E_{50}^{ref}) in the three clay layers, can be optimized. Based on results of parametric studies presented by Finno et al. (2006), the PSR is approximately equal to 1 for the geometry of the excavation and the system stiffness. This result implies that the soil parameters found from the optimization process based on a plane strain simulation are not artificially stiffer as a result of corner stiffening effects (Finno and Calvello 2005).

The support system elements for the FEDC excavation are modeled with anisotropic linear elastic elements: node-to-node beam elements for the bracing and plate elements for the sheet pile wall. Table 3 lists the support system parameters employed in this analysis. The elastic modulus parameters of the sheet-pile wall are not traditional Young's Moduli, but rather directional bending stiffness parameters, E_i, which depend on the material modulus and wall geometry. The bending stiffness in the horizontal direction (E_2) depends on the sheeting interlocks rather than the wall geometry, and it is assumed that the moment of the sheet-pile in the horizontal direction is less than the vertical direction (E_1) by a factor of 20. The horizontal stiffening effect of the wide-flange beam walers was incorporated into the sheet-pile wall elements by increasing the horizontal bending (E_2) and shear moduli (G_{23}) of the wall elements at the waler locations. See Blackburn and Finno (2006) for more details.

The spread footings and structure of the Tech Building was modeled with stiff, linear elastic plate elements for the walls, slabs and footings. The tech basement was simulated by de-activating corresponding elements and a distributed load was applied to the foundation to model the weight of the structure (Blackburn 2005).

Excavation Procedure Modeling Description

The FEDC excavation procedure was modeled with two scenarios: 1) an 'As-Designed', uniform staged construction, with the entire site excavated to prescribed levels and all the supports on the respective levels installed simultaneously (listed in Table 4) and 2) the 'As-Built' construction procedure, where the corners were excavated first, leaving a berm of soil in the center of the site and the support members were installed at separated time periods, depending on the elevation of the excavation (listed in Table 5). In both cases, the sheet-pile wall was 'wished' into place after the initial site grading. This assumption has little impact on computed displacements given the geometry of the excavation (Finno and Tu 2006).

FINITE ELEMENT CALCULATION RESULTS

Analysis of lateral soil deformations

Horizontal soil displacement responses at the locations corresponding to inclinometers along the north and west walls, calculated with the 'As-Built' excavation sequence model of the FEDC excavation, are compared to the observed soil displacement during the excavation in Figure 11. The computed maximum lateral soil displacement for the north and west walls were 16 and 20 mm, respectively. Both maxima occurred at approximate elev. -3 m, ECD. The observed maxima for Inclinometers 1 and 5 were 13 and 15 mm, for the north and west walls, respectively. The maximum observed deep-seated displacement for all inclinometers occurred below the final excavation grade, whereas the maximum calculated displacement occurred above the final excavation grade.

The difference between horizontal soil displacement profiles (both computed and observed) for the north wall and west walls illustrates the influence of the Tech Building structure and basement on the soil response. The effects of the Tech Building footings are noticeable in the difference in soil displacement at upper elevations, whereas the displacement in the clay layers is little affected by the Tech Building loads. In both the observed and computed deformation profiles (shown in Figure 16), the cantilever displacement of the north wall is greatly reduced, when compared to the west wall, due to the reduction of soil pressure caused by the Tech Building basement.

The effects of using an appropriate excavation sequence model is shown in Figure 17, which shows the computed horizontal soil deformation profiles for both excavation sequence models. While both models overpredict the lateral soil displacement in the upper strata, the FEDC sequence model better predicts the maximum displacement, particularly in the soft, Blodgett clay layer. The maximum calculated soil deformation for the FEDC excavation sequence is approximately 15 mm, whereas the maximum soil displacement for the simplified excavation sequence is approximately 18 mm. The simplified excavation sequence model overpredicted the maximum deformation by 34% and the FEDC excavation sequence overpredicted the maximum deformation by 9%, indicating the increased accuracy of a prediction with proper simulation of construction procedures. Both computed results predict that the maximum movement occurred at a higher elevation than the location of the observed maximum.

ABOVE NEEDS TO BE EVALUATED IN LIGHT OF RESULTS OF FE WANT TO SEE IF N-W AND N-E CORNERS RESPOND AS IN FIGURES 6 AND 7

Analysis of internal bracing responses

Figure 13 compares the computed strut loads for the two excavation sequencing models with the observed earth loading during the FEDC excavation. The 'As-Designed' excavation sequence resulted in strut loads that were smaller than observed in the lower level supports and larger than observed in the upper supports. These comparisons are made after subtracting the temperature-induced axial forces from the observed values, since temperature effects on the structural responses are not included in the finite element formulation. *However, the cumulative loads, defined as the sum of both top and bottom support loads, for supports T/B-3,4 and 6 were reasonable. The cumulative loading in the small corner diagonals is underpredicted for both* *sequence scenarios (Blackburn, 2005).* THIS DEPENDS ON WHAT T-5 LOOKS LIKE AFTER REMOVING BAD GAGE DATA

The 'As-Constructed' excavation sequence model prediction shows a closer match to the observed cross-lot earth loading (T/B-3 and 4) and a good match for the medium and large diagonal members. The close match between observed axial earth loading and the computed axial loads for the 'As-Constructed' excavation sequence (compared to the 'As-Designed' sequence) and the slightly better computation of maximum lateral movements demonstrate the importance of accurately modeling the excavation sequence during design procedures.

CONCLUSIONS

Based on results of the field observations and three-dimensional finite element computed results presented herein, the following conclusions can be drawn:

While the deep-seated movements varied between 0.19 and 0.26% of the excavated depth and thus were typical of those expected for the conditions at the site, the movements in the upper 5 m reflect the influence of the lower ground surface elevation on the north side of the support system and the effects of the adjacent basement. Cantilever movements of 35 and 28 mm were observed at the higher sides of the excavation in the east (I-3) and west inclinometers (I-5) , respectively. These walls rotated about the second support level, rather than the first level, as is typically observed. These cantilever movements imply that the diagonal bracing transfers the loads from the higher east and west sides to the lower north side and thus minimizing cantilever displacements along the north side.

Axial loads in the upper level of bracing changed little when the lower level bracing was installed, in contrast to the typical response where the load drops significantly when a lower brace level is installed. Results of finite element simulations indicate that these responses were caused by the non-uniform excavation sequence. The axial loads in the bracing were larger than those computed using the Teraghi and Peck apparent earth pressure diagram, in large part because of the temperature-induced axial loads.

According to the classification of Burland and Wroth (1975), The support system and excavation sequence at the FEDC resulted in negligible damage to the adjacent building supported on shallow foundations. The slight cracking that did occur was located in the area where the stiffening effects of the corner of the excavation impacted the deformations surrounding the excavation.

ACKNOWLEDGEMENTS

Financial support for this work was provided by National Science Foundation grant CMS-0219123 and the Infrastructure Technology Institute (ITI) of Northwestern University. The support of Dr. Richard Fragaszy, program director at NSF, and Mr. David Schulz, ITI's director, is greatly appreciated. Cone penetration test data were provided by Dr. Paul Mayne's research group at Georgia Institute of Technology. Special thanks to Phil Blakeman of Turner Construction, Michael Wysockey of Thatcher Engineering, Jay Baehr of Northwestern University Facilities Management, Robert Acker of STS Consultants for granting site access and providing data. Additional assistance was provided by current and past Northwestern University graduate and undergraduate students: Jill Roboski, Terrance Holman, Cecelia Rechea, Wan-Jei Cho, and Kate Sylvester.

REFERENCES

Blackburn, J.T. (2005). “Automated remote sensing and three-dimensional analysis of internally braced excavations,” PhD Dissertation, Dept. of Civil Engineering, Northwestern University, Evanston, IL.

Blackburn, J.T., Sylvester, K. and Finno, R.J. (2005). "Observed bracing responses at the Ford Design Center excavation." *Proc. 16th International Conf. on Soil Mechanics and Geotechnical Engineering*, Osaka, Japan, 2005.

Bono, N.A., Liu, T.K., and Soydemir, C. (1992). “Performance of an Internally Braced Slurry-Diaphragm Wall for Excavation Support.” *Slurry Walls: Design, Construction, and Quality Control, ASTM STP 1129*, David B. Paul, Richard G. Davidson, and Nicholas J. Cavalli, Eds., ASTM, Philadelphia.

Boone, S.J. and Crawford, A.M. (2000). “Braced Excavations: Temperature, Elastic Modulus, and Strut Loads.” *J. of Geotech. and Geoenv. Engrg.,* ASCE, 126(10), 870-881.

Burland, J. B., and Wroth, C. P. (1975). “Settlement of Buildings and Associated Damage.” *Proceedings of a Conference on Settlement of Structures*, Cambridge, 611-654.

Chew, S. H., Yong, K. Y., and Lim, A. Y. K., (1997). “Three-dimensional finite element analysis of a strutted excavation,” *Computer Methods and Advances in Geomechanics*, Yuan (editor), Balkema, Rotterdam.

Clough, G. W., Smith, E. M., and Sweeney, B. P. (1989). “Movement Control of Excavation Support Systems by Iterative Design.” *Current Principles and Practices, Foundation Engineering Congress*, Vol. 2, ASCE, 869-884.

Finno, R.J. and Blackburn, J.T. (2005). “Automated Monitoring of Supported Excavations.” Proc. of *13th Annual Great Lakes Geotechnical and Geoenvironmental Engineering Conference*, ASCE Geotechnical Practice Publication No. 3, ed. H.H. Titi, May 13, 2005, Milwaukee, WI.

Blackburn, J.T. and Finno, R.J. (2006). “Representing internal bracing systems in 3-D models of deep excavations.” *Proc. GeoCongress 2006*, February, 2006, Atlanta, GA.

Finno, R.J., Blackburn, J.T., and Roboski, J.F. (2006). " Three-dimensional Effects for Supported Excavations in Clay.” Submitted to *J. of Geotech. and Geoenv. Engrg.*, ASCE.

Finno, R. J., Bryson, L. S., and Calvello, M. (2002). “Performance of a stiff support system in soft clay.” *J. of Geotech. and Geoenv. Engrg.*, ASCE, 128(8), 660-671.

Finno, R.J. and Calvello, M. (2005). “Supported Excavations: Observational Method and Inverse Modeling.” *J. of Geotech. and Geoenv. Engrg.,* ASCE, 131(7), 826-836.

Finno, R.J., Nerby, S.M., and Atmatzidis, D.K. (1988)."Ground Response to Sheet Pile Installation in Clay." *Proc. Second Int. Conf. on Case Histories in Geotech. Engrg.*, June 1-5, 1988, St. Louis, MO, 1297-1301.

Finno, R.J. and Roboski, J.F., (2005). "Three-dimensional Responses of a Tied-back Excavation through Clay." *J. of Geotech. and Geoenv. Engrg.*, ASCE, Vol. 131, No. 3, March, 273-282.

Lee, F. H., Yong, K. Y., Quan, K. C., and Chee, K. T. (1998). "Effect of Corners in Strutted Excavations: Field Monitoring and Case Histories." *J. Geotech. Engrg.*, ASCE, 124(4), 339-349.

Lin, D. G., Chung, T. C., and Phien-wej, N. (2003). "Quantitative evaluation of corner effect on deformation behavior of multi-strutted deep excavation in Bangkok subsoil." *Geotechnical Engineering*, 34(1), 41-57.

Ou, C. Y., and Chiou, D. C. (1993). "Three-dimensional finite element analysis of deep excavation." *Proc., 11th Southeast Asian Geotechnical Conf.,* The Institute of Engineers, Malaysia, Kuala Lampur, Malaysia, 769-774.

Ou, C. Y., Chiou, D. C., and Wu, T. S. (1996). "Three-dimensional finite element analysis of deep excavations." *J. Geotech. Engrg.*, ASCE, 122(5), 473-483.

Ou, C.Y., Shiau, B.Y., and Wang, I. W. (2000a). "Three-dimensional deformation behavior of the Taipei National Enterprise Center (TNEC) excavation case history." *Canadian Geotechnical Journal*, 37, 438-448.

Ou, C.Y., Liao, J.T., and Cheng, W.L. (2000b). "Building response and ground movements induced by a deep excavation." *Geotechnique*, 50(3), pp. 209-220.

Peck, R.B. and Reed, W.C. (1954). "Engineering properties of Chicago subsoils." *Engineering Experiment Station, Bulletin 423*, University of Illinois at Urbana –Champaign, Urbana, IL.

Plaxis (2004), 3D Foundation-Version 1 User Manual. Eds. R.B.J. Brinkgreve & W. Broere, A.A. Belkema Publishers, Lisse.

Rechea, C. (2006). Ph.D. Dissertation, Dept. of Civil Engineering, Northwestern University. Evanston, IL.

Schanz T., Vermeer P.A. and Bonnier P.G. (1999). "The Hardening Soil model -formulation and verification." Proceedings Plaxis Symposium *Beyond 2000 in Computational Geotechnics*, Amsterdam, Balkema, 281-296.

Terzaghi, K. and Peck, R.B. (1967). Soil Mechanics in Engineering Practice, 2nd Edition, John Wiley and Sons, New York, New York.

Wong, L. W. and Patron, B. C. (1993). “Settlements induced by deep excavations in Taipei.” *Eleventh Southeast Asian Geotechnical Conference*, Singapore.

FROM 3-D PAPER

Chew, S. H., Yong, K. Y., and Lim, A. Y. K., 1997. “Three-dimensional finite element analysis of a strutted excavation,” *Computer Methods and Advances in Geomechanics*, Yuan (editor), Balkema, Rotterdam.

Clough, G. W., Smith, E. M., and Sweeney, B. P. 1989. Movement Control of Excavation Support Systems by Iterative Design. *In* Current Principles and Practices, Foundation Engineering Congress, Vol. 2. ASCE, pp. 869-884.

Finno, R. J., and Bryson, L. S. 2002. Response of a building adjacent to stiff excavation support system in soft clay. Journal on the Performance of Constructed Facilities, ASCE, 16(1): 10-20.
Finno R.J., Bryson L.S. and Calvello M. (2002). Performance of a stiff support system in soft clay. Journal of Geotechnical and Geoenvironmental Engineering, ASCE, Vol. 128, No. 8, p. 660-671.

Finno, R. J., and Roboski, J. F. 2005. Three-dimensional response of a tied-back excavation through clay. Journal of Geotechnical and Geoenvironmental Engineering, ASCE. 131(3): 273-282.

Lee, F. H., Yong, K. Y., Quan, K. C., and Chee, K. T. 1998. Effect of Corners in Strutted Excavations: Field Monitoring and Case Histories. J. Geotech. Engrg., ASCE, 124(4), 339-349.
Lin, D. G., Chung, T. C., and Phien-wej, N. 2003. Quantitative evaluation of corner effect on deformation behavior of multi-strutted deep excavation in Bangkok subsoil. Geotechnical Engineering, 34(1), 41-57.

Ou, C. Y., and Chiou, D. C. 1993. Three-dimensional finite element analysis of deep excavation. Proc., 11th Southeast Asian Geotechnical Conf., The Institute of Engineers, Malaysia, Kuala Lampur, Malaysia, 769-774.

Ou, C. Y., Chiou, D. C., and Wu, T. S. 1996. Three-dimensional finite element analysis of deep excavations. J. Geotech. Engrg., ASCE, 122(5), 473-483.

Ou, C.Y., Shiau, B.Y., and Wang, I. W. (2000a). “Three-dimensional deformation behavior of the Taipei National Enterprise Center (TNEC) excavation case history,” Canadian Geotechnical Journal, 37, 438-448.

Ou, C.Y., Liao, J.T., and Cheng, W.L. (2000b). Building response and ground movements induced by a deep excavation. *Geotechnique.* 50(3): 209-220.

Roboski, J.F. and Finno, R.J., (2006). Distributions of Ground Movements Parallel to Deep Excavations, Canadian Geotechnical Journal. in press.

List of tables

Table 1. Construction stages at FEDC excavation
Table 2. Soil parameters used in finite element analyses
Table 3. Wall and waler parameters used in finite element analyses
Table 4. "As-designed" excavation sequence used in finite element analysis
Table 5. "As-constructed" excavation sequence used in finite element analysis

List of figures

Figure 1. Excavation plan and instrument locations
Figure 2. Subsurface conditions
Figure 3. Excavation photographs
Figure 4. Lateral movements caused by installing sheet-pile wall
Figure 5. Lateral soil movements in soft clay
Figure 6. Lateral soil movements in northwest corner
Figure 7. Lateral soil movements in northeast corner
Figure 8. Location of exterior cracks in adjacent building
Figure 9. Observed and earth-pressure induced strut loads
Figure 10. Detailed inset and cross-section of 3-D finite element mesh
Figure 11. Computed and observed lateral movements at north and west sides of excavation
Figure 12. Computed lateral movements for "as-built" and "as-designed" simulations
Figure 13. Computed and "observed" strut loads

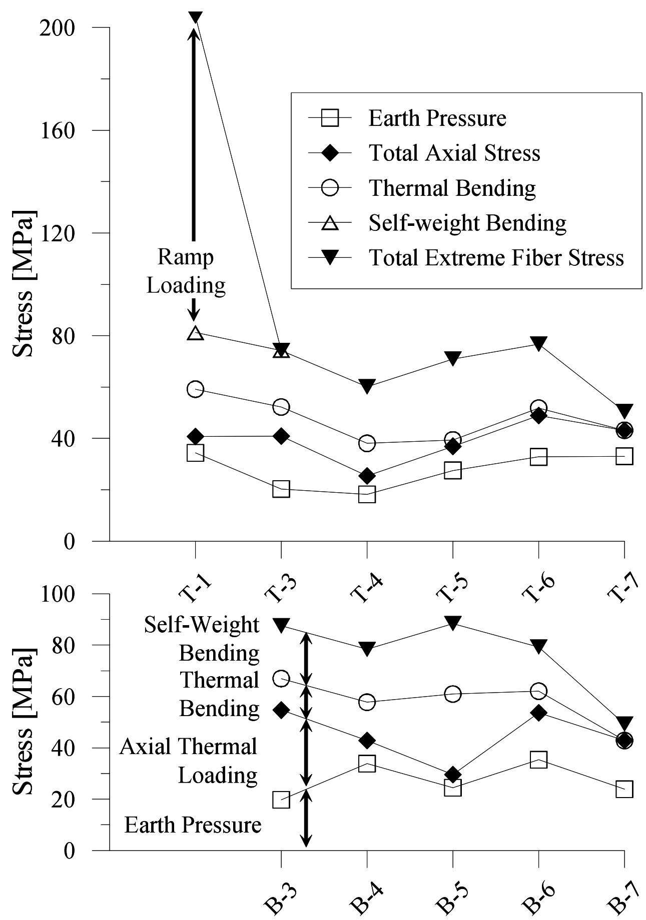

200
160
120
80
40
0
Stress [MPa]
Ramp Loading
Earth Pressure
Total Axial Stress
Thermal Bending
Self-weight Bending
Total Extreme Fiber Stress
T-1
T-3
T-4
T-5
T-6
T-7
100
80
60
40
20
0
Stress [MPa]
Self-Weight Bending
Thermal Bending
Axial Thermal Loading
Earth Pressure
B-3
B-4
B-5
B-6
B-7